Synthesis and characterization of intercalated conducting polymers into modified clay

C. Bouabida, A. Yahiaoui*, A. Hachemaoui. A. M. Benkouider

Laboratoire de Chimie Organique, Macromoléculaire et des Matériaux, Université de Mascara, Mascara 29000, Algeria.

Abstract

We account preparation and structural, of Poly (Aniline-co-N-ethylaniline)/montmorillonite nanocomposites in different molar ratio by chemical oxidative polymerization. The developed nanocomposites were characterized using various analytical techniques such as X-ray diffraction (XRD), Fourier transform infrared (FT-IR), UV-Vis spectroscopy and cyclic voltammetry spectroscopy. The results were compared with rude montmorillonite. The intensity of diffraction peaks for MMT/Poly (AN-co-NEA) composites are lower than that for montmorillonite. These observed effects have been attributed to interaction of clay with PANi,PNEA and Poly(AN-co-NEA) molecular chains. Both FTIR and UV-Vis studies of the composites revealed that there is a strong interaction between polymer matrix and clay,and the cyclic voltammetry indicate the electroactive effect of nanocomposite increased with aniline in the polymer chain.

Keywords: Nanocomposite, Conducting polymers, Montmorillonite, Characterization, Green Chemistry

1. Introduction

Recently organic/inorganic hybrid materials become one of the most extensively studied material all over the world. Its main reason is to expect, to be obtained new class of composite materials with synergetic or complementary behaviors, and it is used in electronic nanoelectronic and biomedical devices [1-6].Moreover nanocomposite material composed of conducting polymers & clay, which opened more fields of applications [7, 8] such as drug delivery [9, 10]. The conducting polymers interest a great scientific and technological importance because of their unique electrical, electronic, magnetic and optical properties [11-14].

Among the conducting polymers, conducting polyaniline (PANI) is often used as an organic part to prepare nanocomposites because of its low cost, easy preparation, controllable unique properties by oxidation and protonation state, excellent environmental stability and potential application such as light emitting diodes, transparent electrodes, electromagnetic radiation shielding, corrosion protection of metals, battery, gas and humidity sensing purposes. [15]. Nanoscale conjugated organic molecules and polymers can be used for biosensors, electrochemical devices, single electron transistors, nanotips of field emission display, etc. [16-20].

Montmorillonite is one of those inorganic materials. It has been attracted a great attention due to its remarkable improvement in mechanical, thermal, flame-retardant, and barrier properties of polymeric composites with small amounts (1–10 wt.%) of MMT fillers added [21]. These properties improve the nanometric thickness and high aspect ratio of the individual clay platelets, as well as, the nanocomposite morphology with the platelets being exfoliated and well-dispersed [22]. It is regularly used for packaging and medical applications [23-25]. Feng et al. and Kwon et al. have successfully demonstrated MMT as useful for biomedical application [23, 24].

This paper will also discuss the synthesis and the characterization of MMT/Poly (AN-co-NEA) nanocomposites by in–situ chemical oxidative polymerization method, which gives very important results.

2. **Experimental**

2.1. *Materials*

Aniline (ANI) and N-ethylaniline (NEA) were purchased from Aldrich chemical company, the water employed for the preparation of the solutions was obtained from an Elga Labwater Purelab Ultra system. Ammonium peroxydisulfate (from merck), NaCl aqueous solution were applied to prepare the modified montmorillonite (M-Na), Ammonium peroxydisulfate (from merck), 'the montmorillonite clay named Maghnite'obtained from Tlemcen (Algeria) has been used.

2.2 *Chemical Synthesis of nanocomposites*

The clay, which has been used, is supplied by a local company known as ENOF Maghnia (Western of Algeria). The clay samples were washed with distilled water to remove impurities; the raw-montmorillonite (10g) were crushed for 20 min using a Prolabo ceramic balls grinder. The greatest proton saturation of the <2 mm fractions of clay were obtained by first saturating with Na^+ ions using 1M NaCl solution . They were then dried at 423 K for 24 h and stored in tightly stoppered glass bottles for later use (samples M-Na).

The composition of M-Na was measured by X-ray fluorescence, obtaining the data in Table 1.

Table.1. Elementary compositions of exchanged sodium-montmorillonite.

Compositions wt.(%)	Na_2O	CuO	MgO	Al_2O_3	SiO_2	P_2O_5	CaO	MnO	Fe_2O_3	ZnO	TiO_2	ZrO_2
Rude clay	0.01	-	3.37	24.15	67.66	0.013	0.013	0.17	0.098	2.80	0.013	0.013
M–Na^+	2.66	-	2.60	17.72	72.77	0.01	0.011	0.175	-	1.95	0.011	0.010

To obtain the nanocomposites: 0.022 M of aniline and/or N-ethylaniline monomers were added with molar ratio (50/50) to 0.5 g of the M-Na. The mixtures were stirred with magnetic stirrers at room temperature for 24 h. The chemical polymerization began when 100 ml of 0.5 M ammonium persulfate $(NH_4)_2S_2O_8$ solution was slowly added to the mixture. The reaction was left at room temperature for 24 h. the resulting precipitate was collected on a filter, washed several times with distilled water to remove unreacted monomers and dried under vacuum at 50 ^{0}C for 24 h.

2.3 *Characterization of nanocomposites*

2.3.1 *Uv-visible measurements*

For recording the UV-Vis absorption spectra, a Hitachi U-3000 spectrophotometer was used. The solution of the homo- and co-polymer in N-methyl-2-pyrrolidone (NMP) was used for recording the spectrum.

2.3.2**.** *FTIR analysis*

Fourier transformed infrared (FTIR) spectrum of the sample was recorded by Fourier transform infrared (Bruker Alpha) spectrophotometer. The FTIR spectrum ranged from 4000 to 450 cm^{-1} at a resolution of 4 cm^{-1}.

2.3.3 *cyclic voltammetry*

The electrochemical behaviour of the polymers was studied by cyclic voltammetry after their extraction from the polymer by dissolving in the N-methyl-2-pyrrolidone (NMP). It is known that this kind of conducting polymers is soluble in NMP [12], while the clay remains in solid state. Thus, both components can be separated by filtration. The electrochemical measurements were carried out using a conventional cell of three electrodes. The counter and reference electrodes were a platinum foil and a hydrogen reversible electrode (RHE), respectively. The working electrode was prepared as follows: after the polymer was extracted from the polymer using NMP, 50µL of this

solution were cast over graphite carbon electrodes and the solvent evaporated to create polymeric films on the order of 25-30 μm. The electrolyte used was 1M $HClO_4$ and all experiments were carried out at 50mV/s.

2.3.4. *XRD analysis*
The X-ray diffraction of the powder nanocomposites were taken using a Bruker CCD-Apex equipment with a X-ray generator (Cu Ka and Ni filter) operated at 40kV and 40mA. The scanning speed and the step size were 0.08°/min and 0.05°, respectively. X-ray fluorescence spectroscopy of the powder nanocomposites was made using a Philips PW1480 equipment with a UNIQUANT II software to determine elements in a semi quantitative way.

2.3.5. *X-ray fluorescence spectroscopy*
X-ray fluorescence spectroscopy of the powder nanocomposites was made using a Philips PW1480 equipment with a UNIQUANT II software to determine elements in a semi quantitative way.

3. **Results and discussion**
3.1. *FTIR Spectroscopy*
Fig. 1 show the FT-IR patterns of Montmorillonite (M), M-Na, PANI/M-Na, PNEA/M-Na and Poly(Aniline-co-N-ethylaniline)/M-Na nanocomposites.
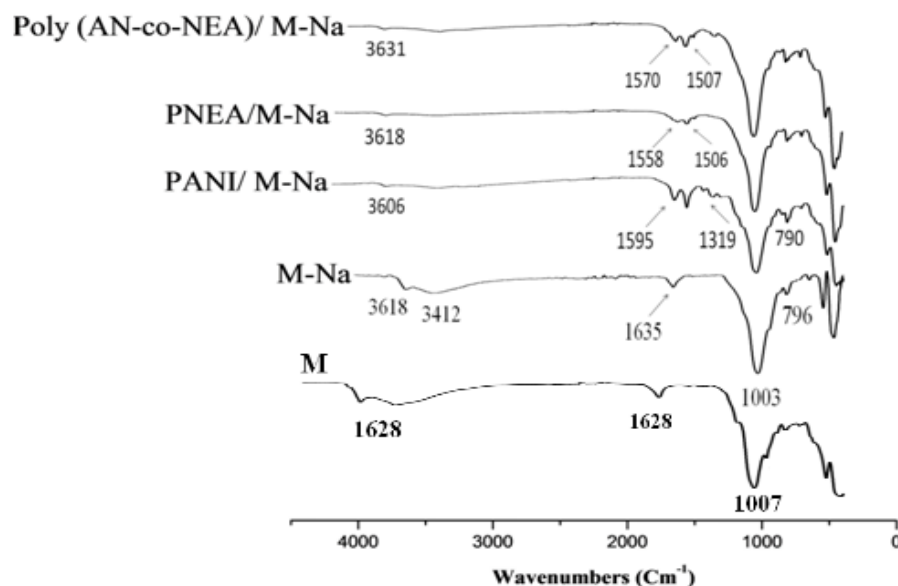

Figure 1: FT-IR adsorption spectra of the: (1) M, (2) M-Na, (3) PANI/ M-Na, (4) PNEA/M-Na and (5) Poly (AN-co-NEA)/ M-Na nanocomposites.

The band betwen 3606 and 3631 cm^{-1} can be attributed to the free (non hydrogen bonded) N–H stretching vibration and hydrogen bonded N-H [26] bond between amine and imine sites, C=N and C=C stretching modes for the quinonoid and benzenoid units occur at 1570 and 1506 cm^{-1} [27,28, 29], the band at 1319 cm^{-1} has been attributed to C-N stretching mode for benzoid unit, while the band at about 790 cm^{-1} is assigned to the in-plane C–H [30,31] bending motions of the aromatic rings.
The bands at 1635 cm^{-1} consist of H–O–H bending of water and at 1003 cm^{-1} is attributed to the Si–O stretching and at 796 cm^{-1} are associated with the Al–O bending.
The FTIR spectra of composites (fig. 1) show that intensities of most of the peaks are affected by the presence of M-Na during polymerization of PANI, PNEA and Poly(AN-co-NEA). This can be explained on the basis of

constrained growth and restricted modes of vibration in polymers grown in presence of M-Na. In this case the monomer gets absorbed on clay and polymerization proceeds initially on the surface of the montmorillonite when ammonium persulphate is added to the solution.

3.2. *UV–vis spectroscopy*
In order to investigate optical properties of fabricated materials, UV–vis spectroscopy was carried out on products. The UV–vis spectrum of PANI/M-Na, PANI/M-Na and Poly (AN-co-NEA)/M-Na nanocomposites are shown in Fig. 2.
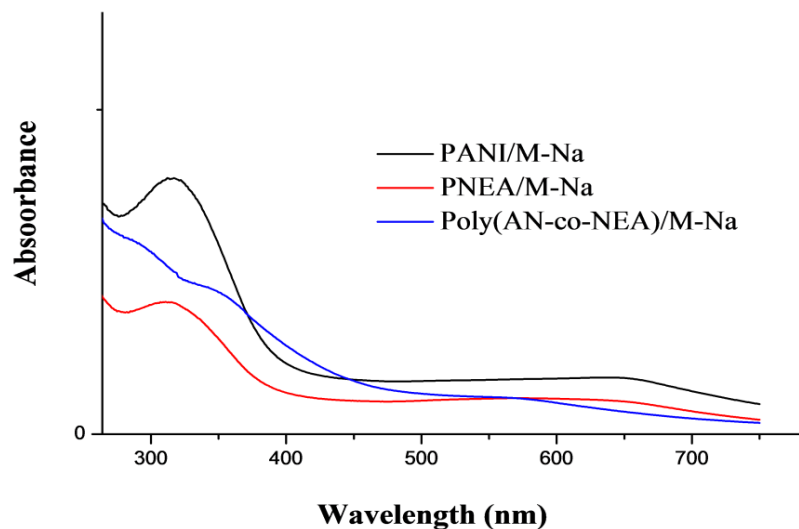

Figure 2: UV–Vis spectra of the: (1) PANI/M-Na, (2) PNEA/M-Na and (3) Poly (AN-co-NEA)/M-Na nanocomposites.

PANI/M-Na has two characterization absorption bands at around 315 nm and 629 nm that attributed to π–π^* transition of the benzenoid ring and n–π^* transition of benzenoid to quinoid, respectively [32].
PNEA/M-Na present two characteristics bands around 313 nm and 608 nm are associated with the excitation of benzenoid to quinoid rings.
In the case of Poly(Aniline-co-N-ethylaniline)/M-Na three bands are present at around 291 nm and 348 nm assigned to π–π^* and at 571 nm assigned to π–π^* du of -N=. This result is in a good agreement with X-ray diffraction patterns of these nanocomposites.

3.2. *XRD spectroscopy*
To confirm the intercalation of PANI into the layers of Na^+-MMT, various kinds of analysis method can be applied. XRD was used to investigate the intercalation of Poly (AN-co-NEA) inside a MMT interlayer as shown in Fig. 3 and Table 2.
    The d-spacing values (d_{001}) were calculated from the peak position of XRD pattern using Bragg's equation $d=2\pi/q$, where q is the magnitude of scattering vector defined as $q= (4\pi/\lambda) \sin (\theta)$; λ is the X-ray wavelength, and 2θ is the scattering angle [33].
The introduction of the polymers had considerable effect on the diffraction pattern.
For the M–Na, a peak, which appears at $2\theta = 7.16$, corresponds to the d-spacing of 12.41 Å. The diffraction peak of PANI and PNEA M–Na, which decreased to a lower angle of $2\theta = 6.11$ Å, and 6.05 Å gave a d-spacing of 14.44 Å and 14.59 Å. The increase of d-spacing was demonstrated to be shifted due to the intercalation of the polyaniline and the poly N-ethylaniline between the M–Na layers [34].
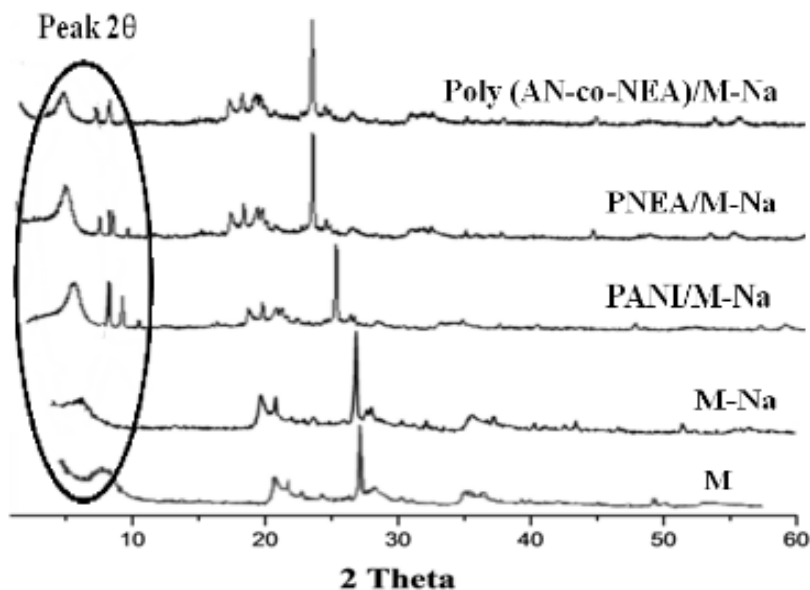
Figure 3: XRD diffraction patterns of Montmorillonite, M–Na,
PANI/ M–Na, PNEA/ M–Na and Poly(AN-co-NEA)/M–Na nanocomposites.

Table 2: Peak maximum and d-spacing of the nanocomposites intercalated into sodium montmorillonite.

Composites	Peak maximum, 2θ max (deg)	Basal spacing, d (001) (Å)	Interlayer spacing, Δd (A°)
M	7.27	11.98	-
M–Na	7.16	12.41	0.43
PANI/M–Na	6.11	14.44	2.03
Poly(NEA)/M–Na	6.05	14.59	2.18
Poly(ANI-co-NEA)/M–Na: (50/50)	5.88	15.11	2.7

In the case of Poly (AN-co-NEA)/M–Na nanocomposite, the signal at $2\theta = 7.16$ Å, which corresponds to the d-spacing of pure (M–Na), is shifted to $2\theta = 5.88$ Å, corresponding to an average interlayer distance of 15.11 Å. The increase of 2.7 Å in the distance between the platelets could be attributed to the intercalation of copolymer chains into the clay galleries.

Yoshimoto et al. observed a similar change in the diffraction peak when they intercalated different amounts of anilinium salts into montmorillonite layers [35]. They attributed it to the existence of two types of conformation of intercalated species controlled by the anilinium concentration [35]. Thus, in a similar way, the polymer/M-Na sample can lead to different structures with different basal spacing.

3.4. *Electrochemical characterization*
Electrochemical behavior of nanocomposites synthesized by chemical method has been tested using cyclic voltammetry studies (Fig. 4).
Cyclic voltammograms of PANI/M-Na show three peaks anodic (at 0.42 V, 0.67 V and 0.82 V) .The cathodic response electrochemical show two peaks (at 0.33 V and 0.63 V). It is well known that PANI exists in three well-defined oxidation states: leucoemeraldine, emeraldine, and pernigraniline. In the leucoemeraldine state all the nitrogen atoms are amines, whereas in pernigraniline the nitrogen atoms are imines.
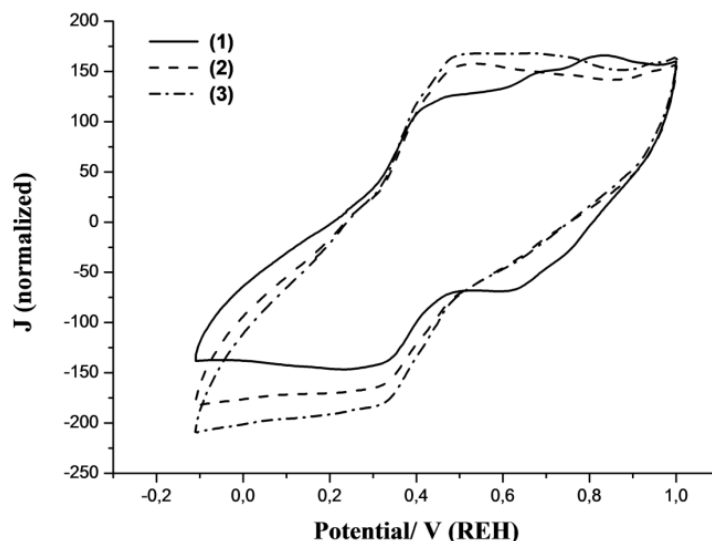
Figure 4: Cyclic voltammograms recorded for a: (1) PANI/M–Na, (2) PNEA/M–Na and (3) Poly(AN-co-NEA)/M–Na nanocomposites.

The cyclic voltammograms of poly N-ethylaniline show two anodic peaks at 0.23 V and 0.49 V. And the cathodic branch display two peaks centred at 0.33 V, 0.89 V
In the case of poly (AN-co-NEA)/M-Na two anodic peaks are observed at 0.25 V, and 0.48 V. And the cathodic response display two intensive peaks centred at 0.32 V, 0.89 V.

Conclusions

A PANI/M-Na, PNEA/M-Na and Poly (AN-co-NEA)/M-Na nanocomposites was successfully obtained by in-situ polymerization and characterized by XRD, UV, FTIR and cyclic voltammetry.
The FTIR and UV results confirmed that there is a strong interaction between polymer chains and the sodium-montmorillonite. Also nanocomposites exhibit well-intercalated structure. The cyclic voltammetry indicate the polymerisation into M-Na is electroactive.

References

1. Schnitzler Da. b C., Meruvia M.S., H˙ummelgen I.A., Zarbin A.J.G., *Chem. Mater*. 15 (2003) 4658-*4665*.
2. Lerari D., Benaboura A., *Mor. J. Chem*. 3 (2015) 202-211.
3. An K.H., Jeong S.Y., Hwang H.R., Lee Y.H., *Adv. Mater*. 16 (2004) 1005–1009.
4. Zengin H., Zhou W., Jin J., Czerw R., Smith D.W., Echegoyen L., Carroll D.L., Foulger S.H., Ballato J., *Adv. Mater*. 14 (2002) 1480-1483.
5. Yong Cao˙ , Guoting Li, Xinbao Li . *Chemical Engeneering journal.* 292 (2016) 207-223.
6. Yasser Zare, Iman Shabani, Materials Science and Engeneering, 60 (2016) 195-203.
7. De Paiva L.B., Morales A.R., Díaz F.R.V., *Appl. Clay Sci*. 42 (2008) 8–24.
8. Jain S., Datta, M., *Appl. Clay Sci.* 104 (2015) 182–188.

9. Li W., Sun L., Pan L., Lan Z., Jiang T., Yang X., Luo J., Li R., Tan L., Zhang S., *Eur. J. Pharm. Biopharm.* 88 (2014) 706–717.
10. Tan D., Yuan P., Annabi-Bergaya, F., Liu D., Wang, L., Liu H., He H., *Appl. Clay Sci.* 96 (2014) 50–55.
11. Retama R.J., *Colloids Surf., A: Phys. Chem. Eng. Asp.* 270–271 (2005) 239–244.
12. Lange U., Roznyatovskaya N.V., M.Mirsky V., *Anal. Chim. Acta* 614 (2008) 1–26.
13. Gupta N., Sharma S., Mir I.A., Kumar D., *J. Sci. Ind. Res.* 65 (2006) 549–557.
14. Cosnier S., *Affinity biosensors, Electroanalysis* 17 (2005) 1701–1715.
15. Huang Jia-xing, VIrji S, Weiller B H, Kaner R B., *Journal of the American Chemical Society*. 125 (2) (2003) 314–315.
16. Azzaoui K., Lamhamdi A., Mejdoubi E., Hammouti B., Berrabah M., Arab. *J. Chem. Environ. Res*. 1 (2014) 41-48
17. Kim B.H., Kim M.S., Kang K.T., Lee J.K., Park D.H., Joo J., Yu S.G., Lee S.H., *Appl. Phys. Lett.* 83 (2003) 539–541.
18. Huang J., *Pure Appl. Chem.* 78 (2006) 15–27.
19. Hatchett D.W., Josowicz M., *Chem. Rev.* 108 (2008) 746–769.
20. Unnati JN., *Maghreb. J. Pure & Appl. Sci*. 2 (2016) 1-16
21. Lee HW, Karim MR, Ji HM, Choi JH, Ghim HD, Park JH, Oh W, Yeum JH., *J Appl Polym Sci* 113 (2009) 1860-1867.
22. Li L, Bellan LM, Craighead HG, Frey MW . *Polymer* 47 (2006) 6208–6217.
23. Feng SS, Mei L, Anitha P, Gan CW, Zhou W ., *Biomaterials* 30 (2009) 3297-306.
24. Kwon SY, Cho EH, Kim SS ., *J Biomed Mater Res Part B Appl Biometer* 83 (2007) 276-284.
25. Angellier-Coussy H, Torres-Giner S, Morel MH, Gontard N, Gastaldi E., *J Appl Polym Sci* 107 (2008) 487-496.
26. Barbero C., Silber J.J., Sereno L. *Journal of electrochemistry*. 263 (1989) 333-352.
27. Tang J., Jing X., Wang B., Wang F., *Syntheic Metals.* 24 (1988) 231-238.
28. Ping Z., Neugebauer H., Neckel A., *Electrochemica Acta*. 41 (1996) 767-772.
29. Zeggai F. Z., Hachemaoui A., Yahiaoui A., J. Mater. Environ. Sci. 6(8) (2015) 2315-2321.
30. Jeevananda T., Seetaramu S., Saravanan S., D'Souza L., *Syntheic Metals*. 140 (2004) 247-260.
31. Turegesean R., Subramanian E., *Materials Chemistry and Physics*. 80 (2003) 731-739.
32. Samrana K., Shahzada A., Jiri P., Josef P., Yyogesh M.J., *J. Materials Science.* 47 (2012) 420-428.
33. Lee D, Lee SH, Char K, Kim J ., *Macromol Rapid Comm* 21 (2000) 1136–1139.
34. Khaldi M., Benyoucef A., Quijada C., Yahiaoui A., Morallo E., *J Inorg Organomet P*. 24 (2014) 267-274.
35. Yoshimoto S., Ohashi F., Kameyama T., *Macromol Rapid Comm*. 25 (2004) 1687-1691.

(2016) ; http://www.jmaterenvironsci.com/